



Supplementary Materials

Supramolecular Porphyrin Nanostructures Based on Coordination-Driven Self-Assembly and Their Visible Light Catalytic Degradation of Methylene Blue Dye

Nirmal Kumar Shee, Min Kyoung Kim and Hee-Joon Kim *

Department of Applied Chemistry, Kumoh National Institute of Technology, Gumi 39177, Korea; nirmalshee@gmail.com (N.K.S.); min1107min@naver.com (M.K.K.)

* Correspondence: hjk@kumoh.ac.kr; Tel.: +82-(54)-4787822

List of contents:

Figure S1. ^1H NMR spectrum of *meso*-5-(4-hydroxyphenyl)-10,15,20-tris(3,5-di-*tert*-butylphenyl)porphyrin in CDCl_3 .

Figure S2. ^1H NMR spectrum of *meso*-(5-(4-hydroxyphenyl)-10,15,20-tris(3,5-di-*tert*-butylphenyl)porphyrinato) zinc(II) in CDCl_3 .

Figure S3. ^1H NMR spectrum of 5,15-bis(3-pyridyl)-10,20-bis(phenyl)porphyrin in CDCl_3 .

Figure S4. ^1H NMR spectrum of *trans*-dihydroxo-(5,10,15,20-tetrakis(3-pyridyl)porphyrinato) tin(IV) in CDCl_3 .

Figure S5. ^1H NMR spectrum of triad **1** in CDCl_3 .

Figure S6. ^1H NMR spectrum of triad **2** in CDCl_3 .

Figure S7. ^1H NMR spectrum of triad **3** in CDCl_3 .

Figure S8. ^1H NMR spectrum of triad **4** (2 mM) in CDCl_3 .

Figure S9. ESI-MS spectrum of triad **1**.

Figure S10. ESI-MS spectrum of triad **2**.

Figure S11. ESI-MS spectrum of triad **3**.

Figure S12. ESI-MS spectrum of triad **4**.

Figure S13. SEM images for the aggregates of triads: (a) **1**; (b) **2**; (c) **3**; (d) **4**.

Figure S14. Particle analyzing data for triad **2** in a *n*-hexane solution.

Figure S15. SEM images of the aggregates of the monomers: (a) ZnL^1 ; (b) SnL^2 .

Figure S16. Absorption spectral changes of triad **4** upon the addition of pyrrolidine in CHCl_3 .

Figure S17. Fluorescence intensity changes of triad **4** upon the addition of pyrrolidine in CHCl_3 .

Figure S18. SEM image for the aggregates of triad **4** upon the addition of pyrrolidine.

Figure S19. Absorption spectra of MB in presence of nano fibers derived from triad **4** under visible light irradiation.

Figure S20. Kinetics for the photocatalytic degradation of MB under visible light irradiation of the four triads (**1**, **2**, **3**, and **4**).

Figure S21. PXRD data of triad **4** before and after an experiment on the photo-degradation of MB.

Figure S22. Catalytic cycles using triad **4** as a photocatalyst for the degradation of MB.

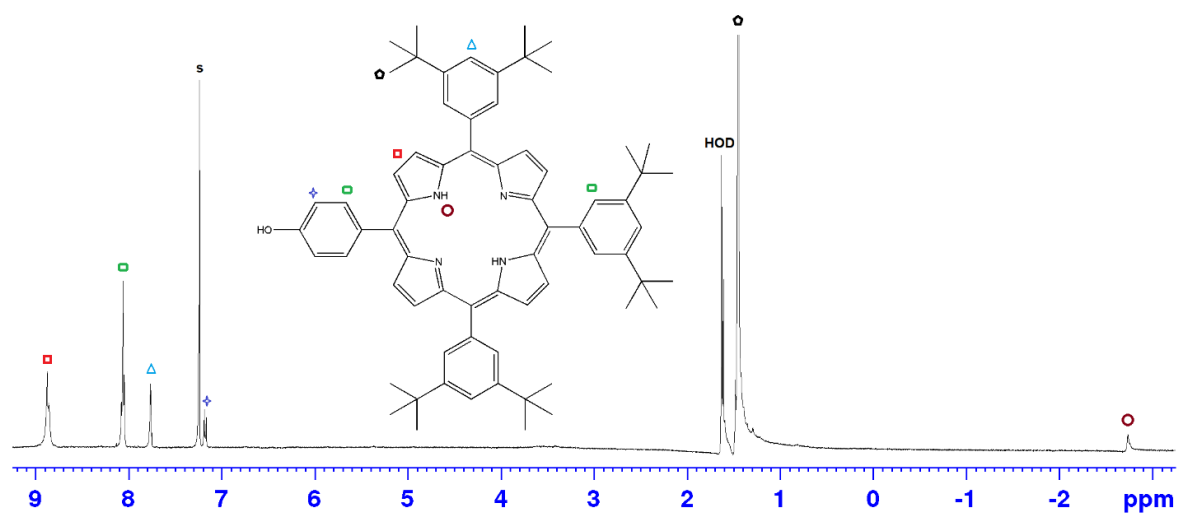


Figure S1. ^1H NMR spectrum of *meso*-5-(4-hydroxyphenyl)-10,15,20-tris(3,5-di-*tert*-butylphenyl)porphyrin in CDCl_3 .

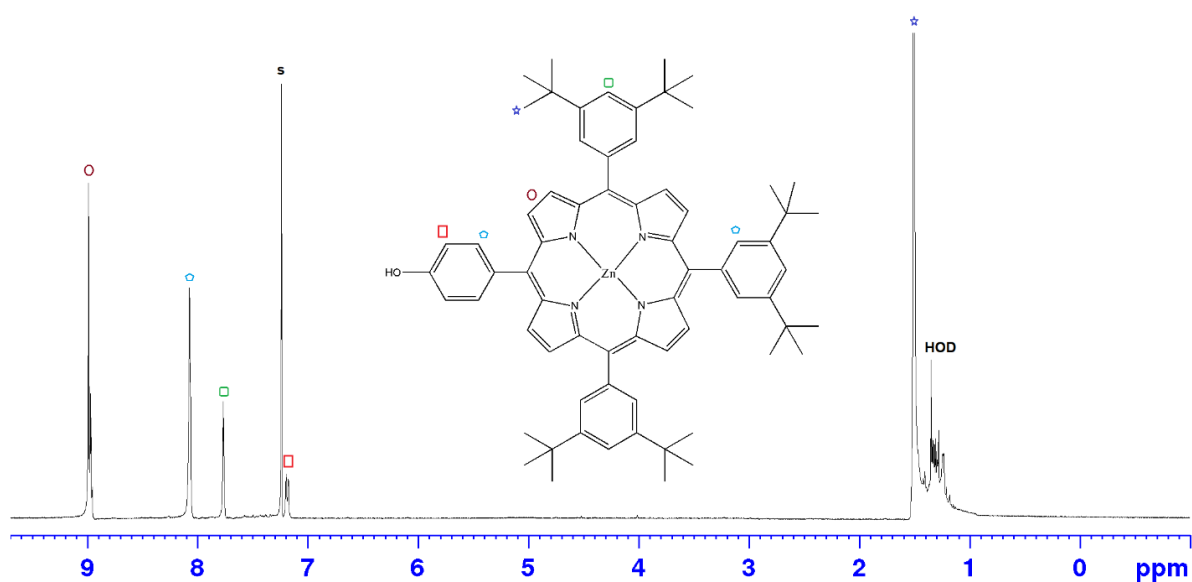


Figure S2. ^1H NMR spectrum of *meso*-(5-(4-hydroxyphenyl)-10,15,20-tris(3,5-di-*tert*-butylphenyl)porphyrinato) zinc(II) in CDCl_3 .

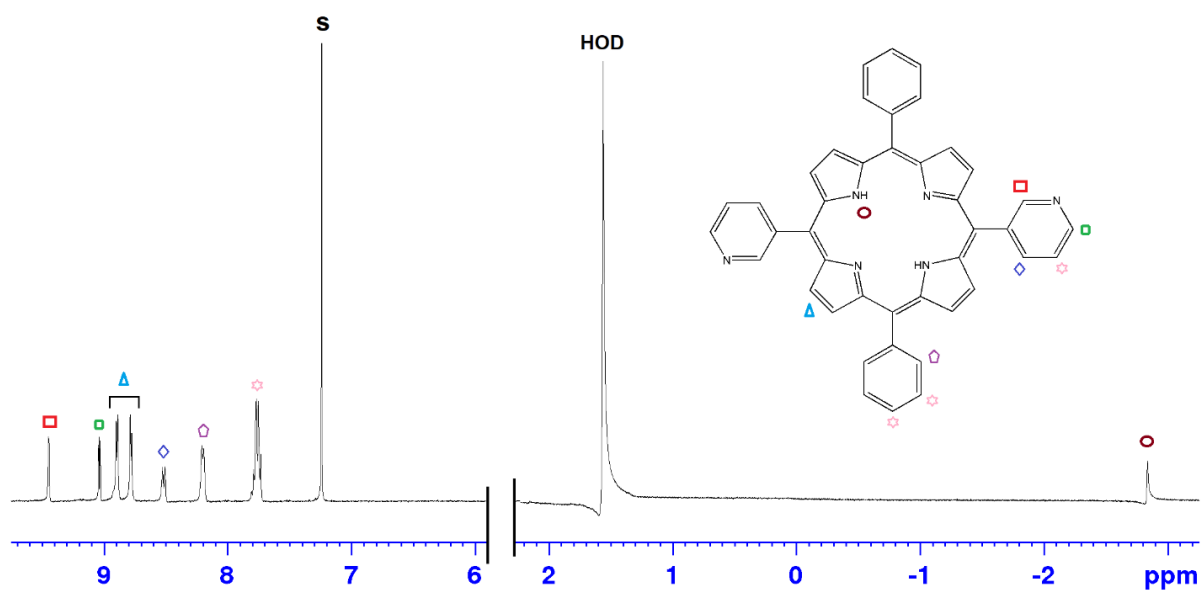


Figure S3. ^1H NMR spectrum of 5,15-bis(3-pyridyl)-10,20-bis(phenyl)porphyrin in CDCl_3 .

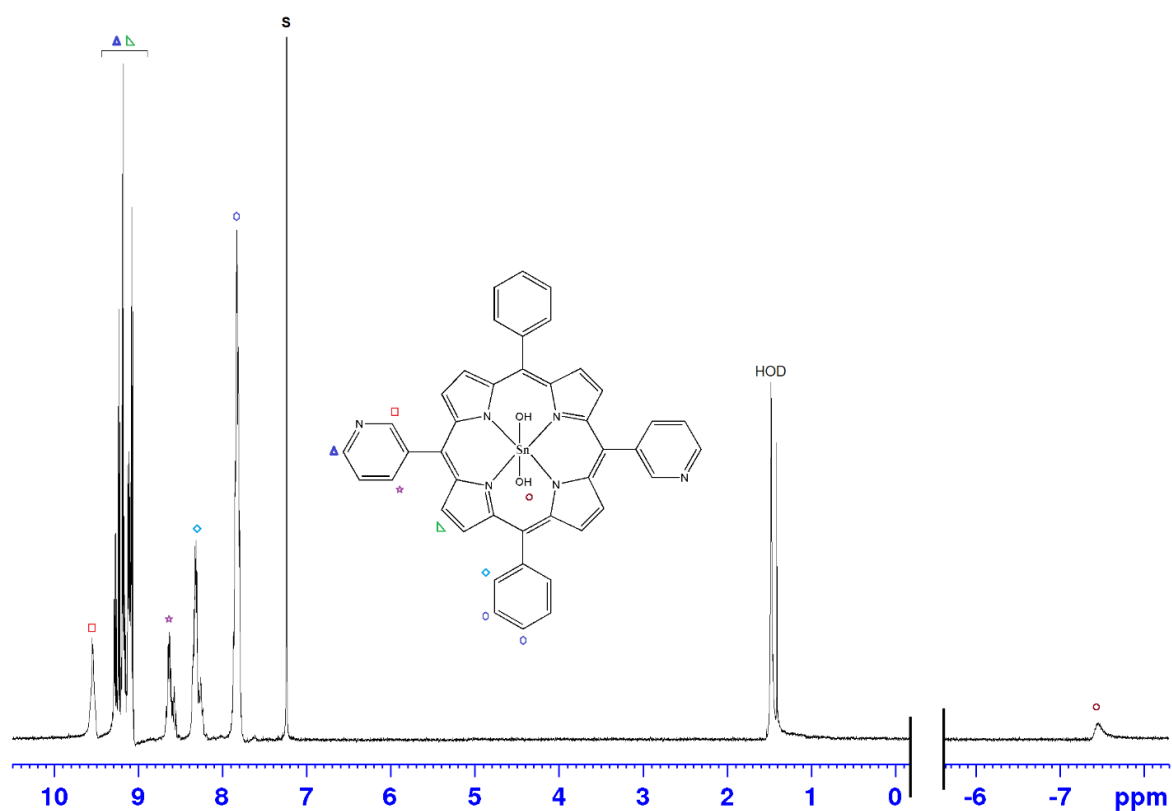


Figure S4. ^1H NMR spectrum of *trans*-dihydroxo-(5,10,15,20-tetrakis(3-pyridyl)porphyrinato) tin(IV) in CDCl_3 .

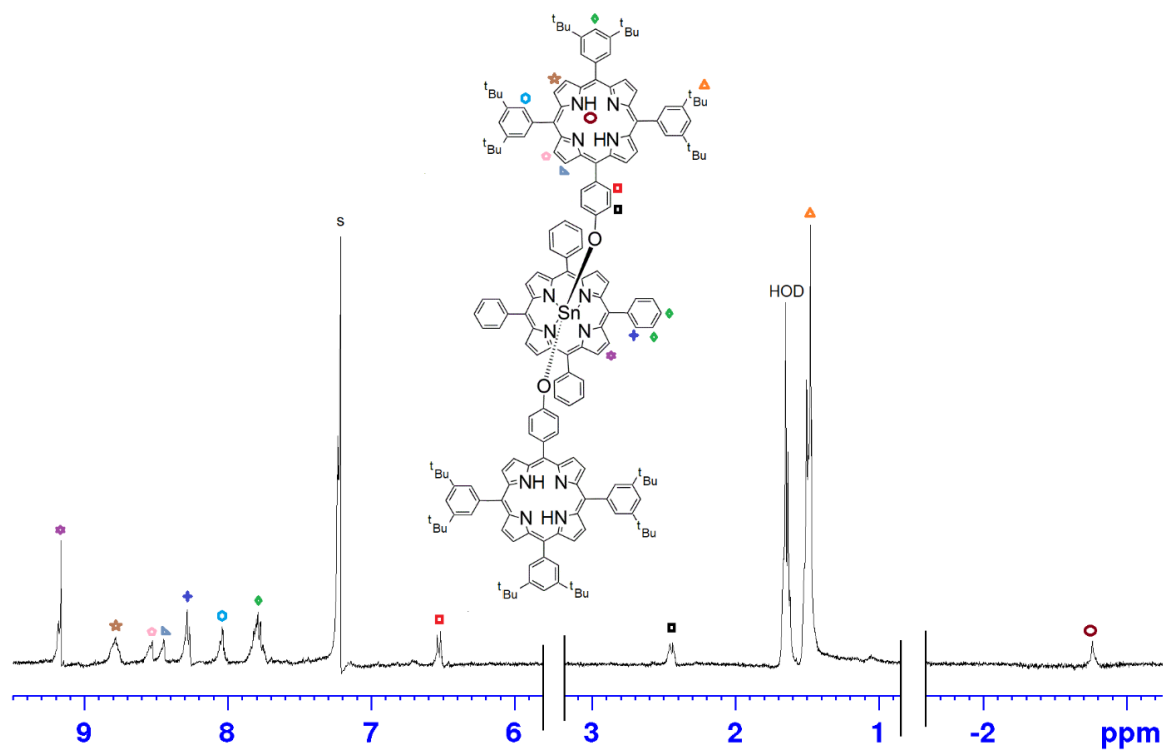


Figure S5. ^1H NMR spectrum of triad 1 in CDCl_3 .

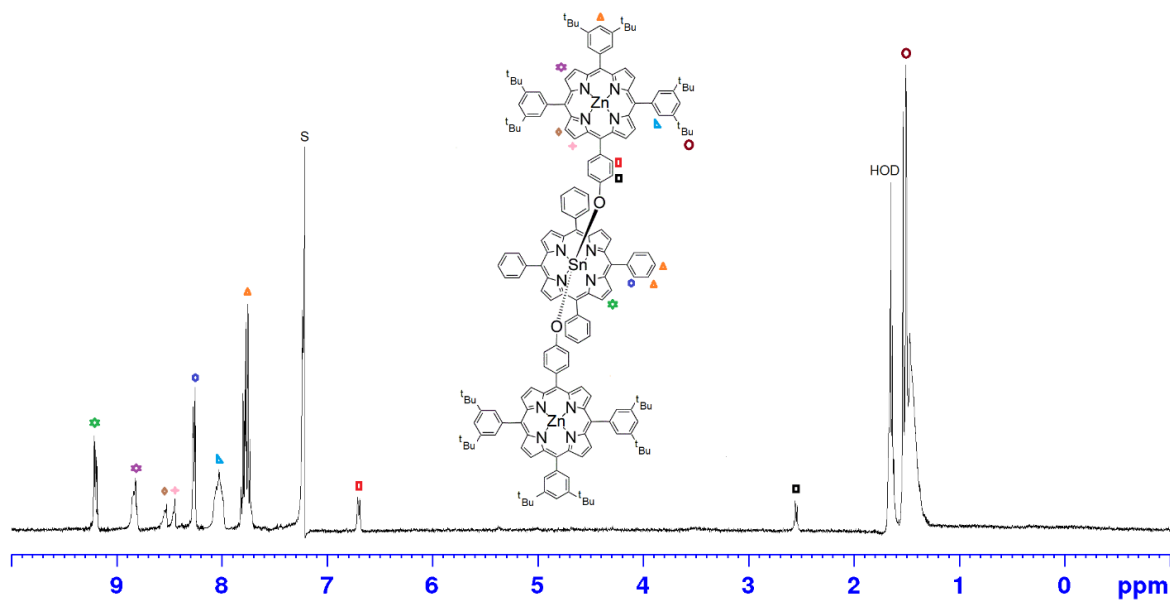


Figure S6. ^1H NMR spectrum of triad 2 in CDCl_3 .

The ^1H NMR spectrum (400 MHz, CDCl_3) of the Zn-Sn complex is displayed. The chemical structure of the complex is shown, with atoms labeled a, b, and c. The spectrum features several peaks corresponding to the complex's protons, with a small inset showing the pyridine ring structure and its labeling.

Figure S8. ^1H NMR spectrum of triad **4** (2 mM) in CDCl_3 after adding 2 eq. pyridine- d_5 (as the solubility of triad **4** in CDCl_3 is very low). In the presence of bases such as pyridine, triad **4** becomes much soluble in CDCl_3 . Residual solvent peaks of pyridine coordinated with Zn porphyrin were assigned as a, b, and c respectively.

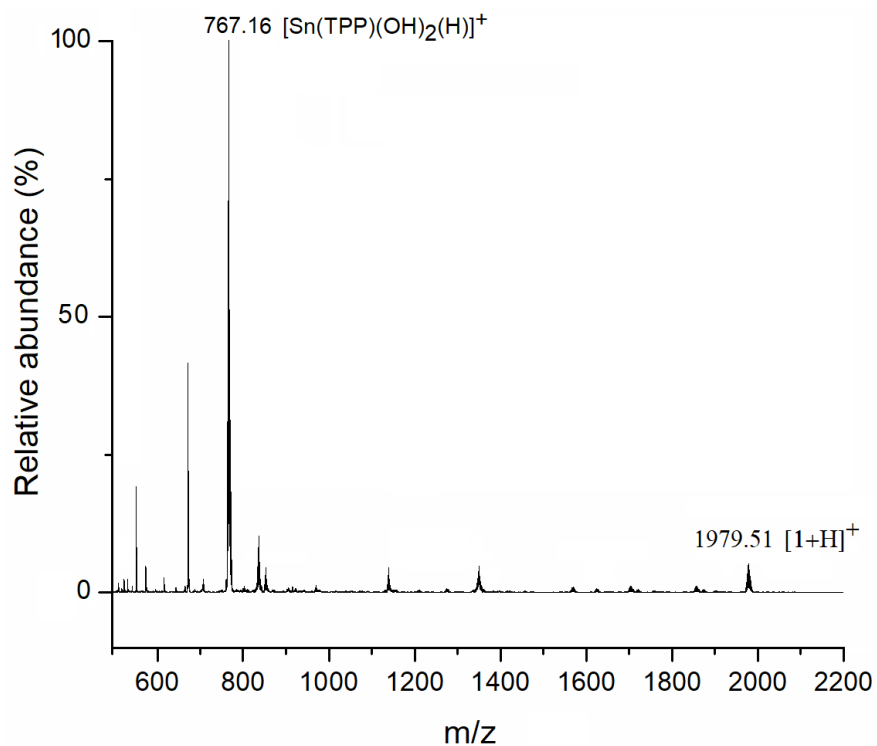


Figure S9. ESI-MS spectrum of triad 1.

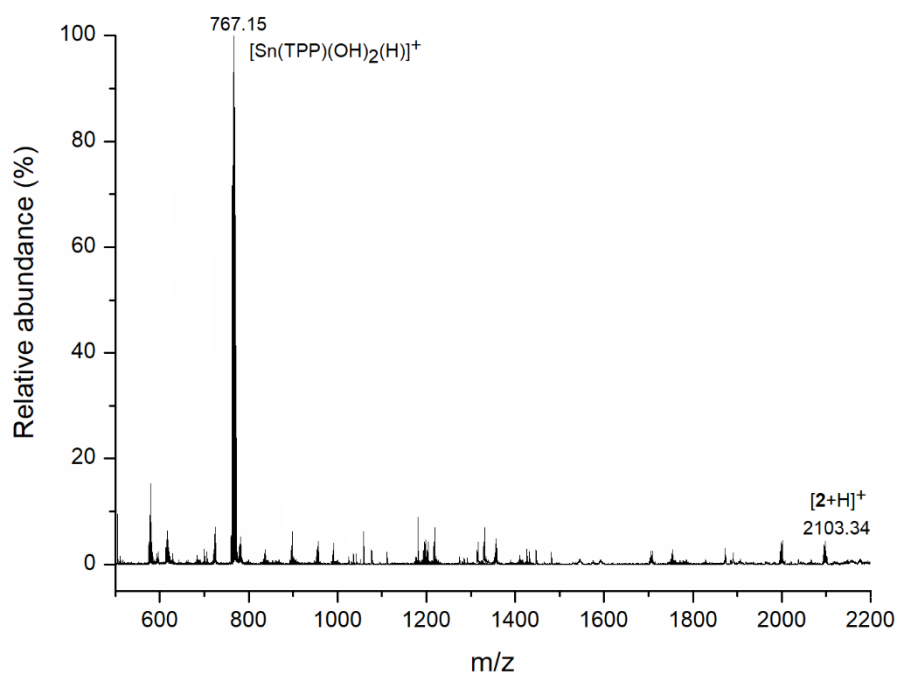


Figure S10. ESI-MS spectrum of triad 2.

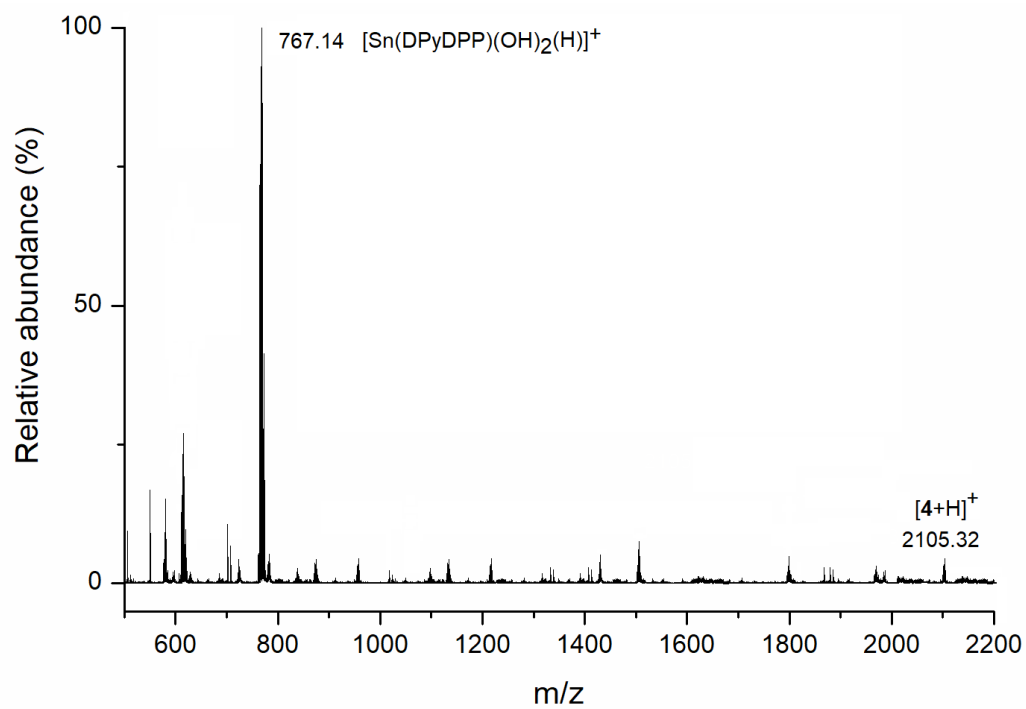


Figure S11. ESI-MS spectrum of triad 3.

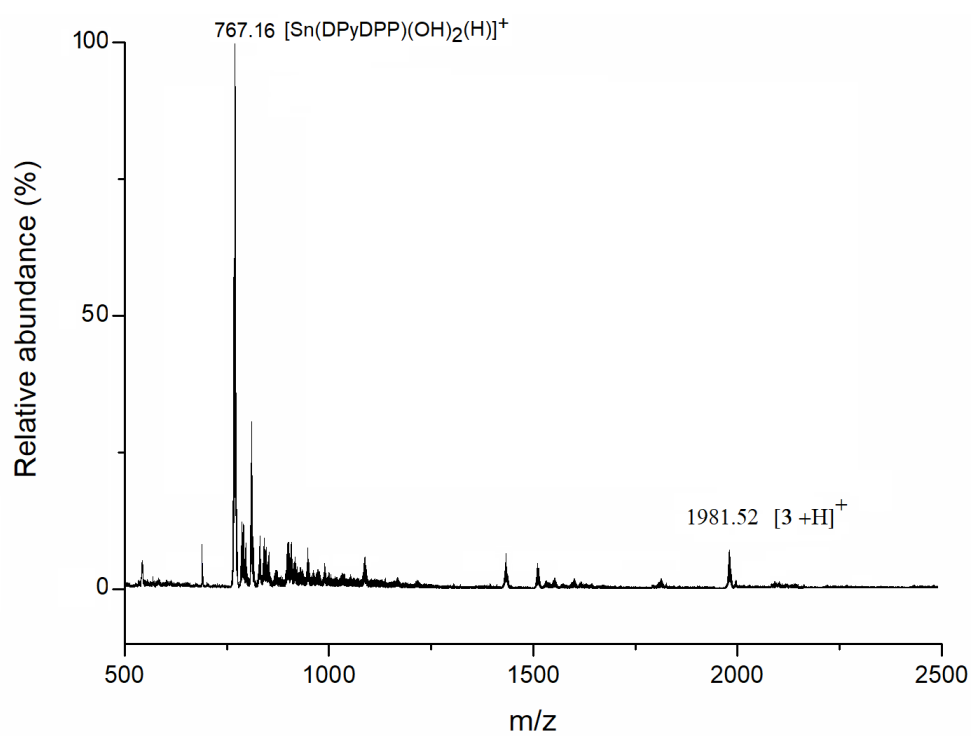


Figure S12. ESI-MS spectrum of triad 4.

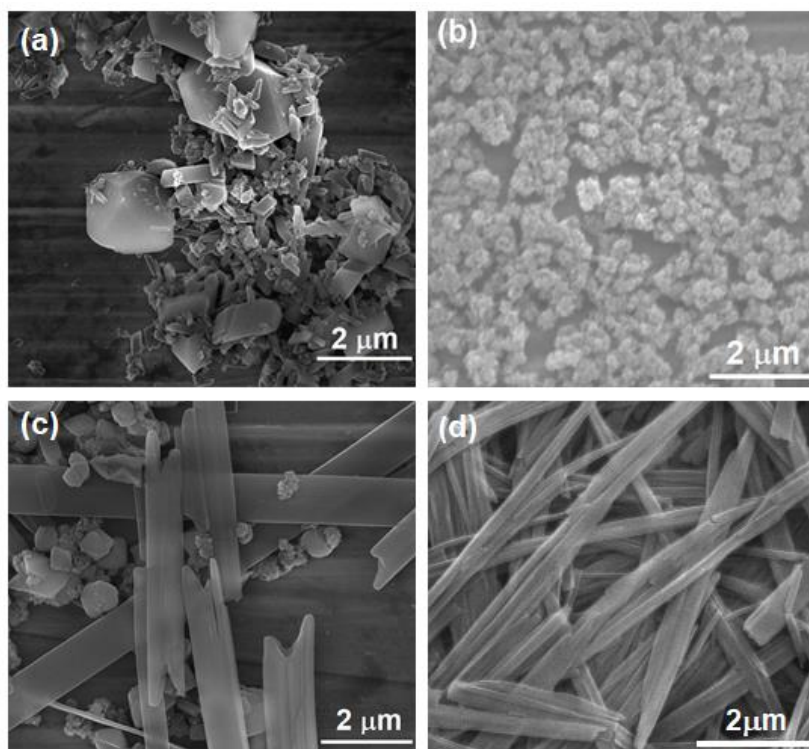


Figure S13. SEM images for the aggregates of triads: (a) 1; (b) 2; (c) 3; (d) 4.

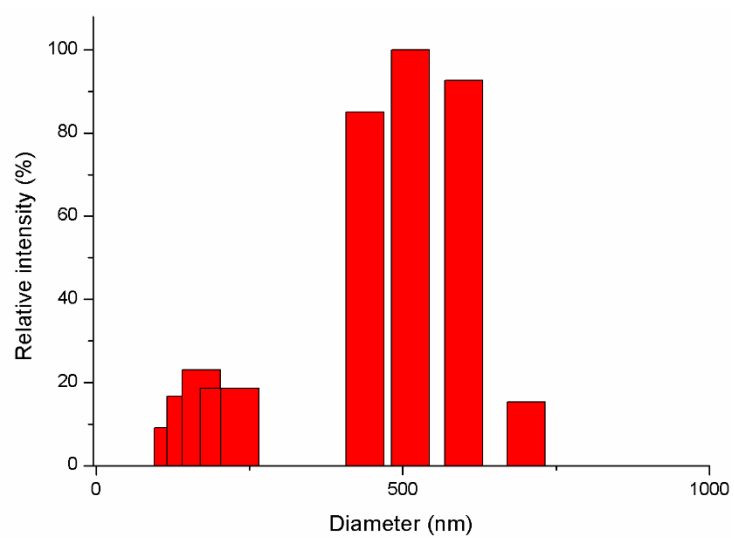


Figure S14. Particle analyzing data for triad 2 in a *n*-hexane solution.

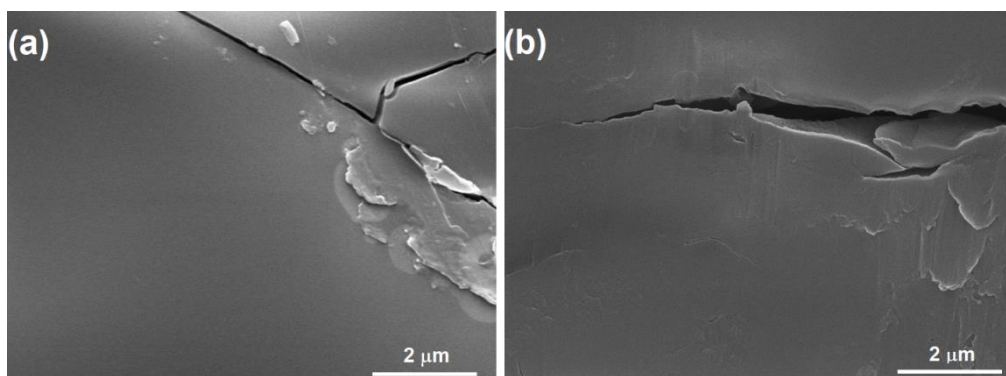


Figure S15. SEM images for the aggregates of the monomers: (a) ZnL¹; (b) SnL².

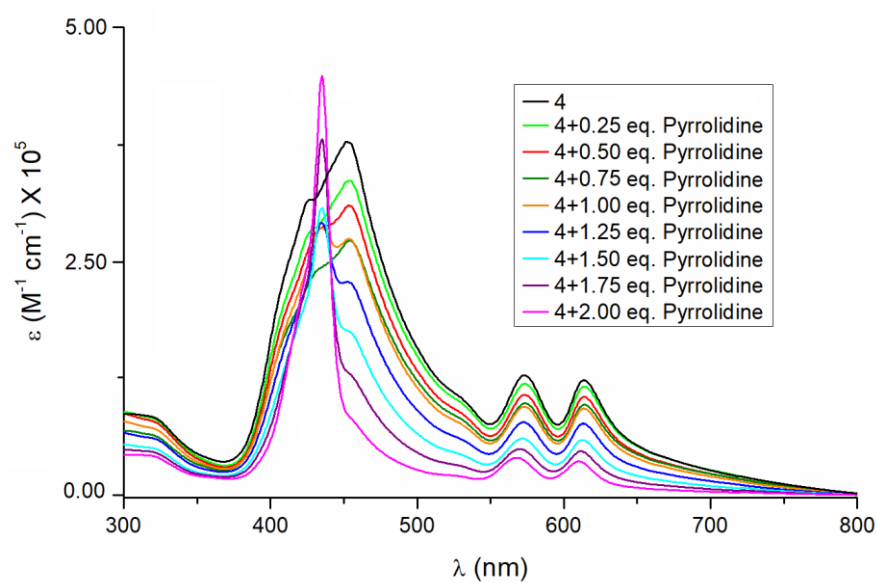


Figure S16. Absorption spectral changes of triad 4 upon the addition of pyrrolidine in CHCl₃.

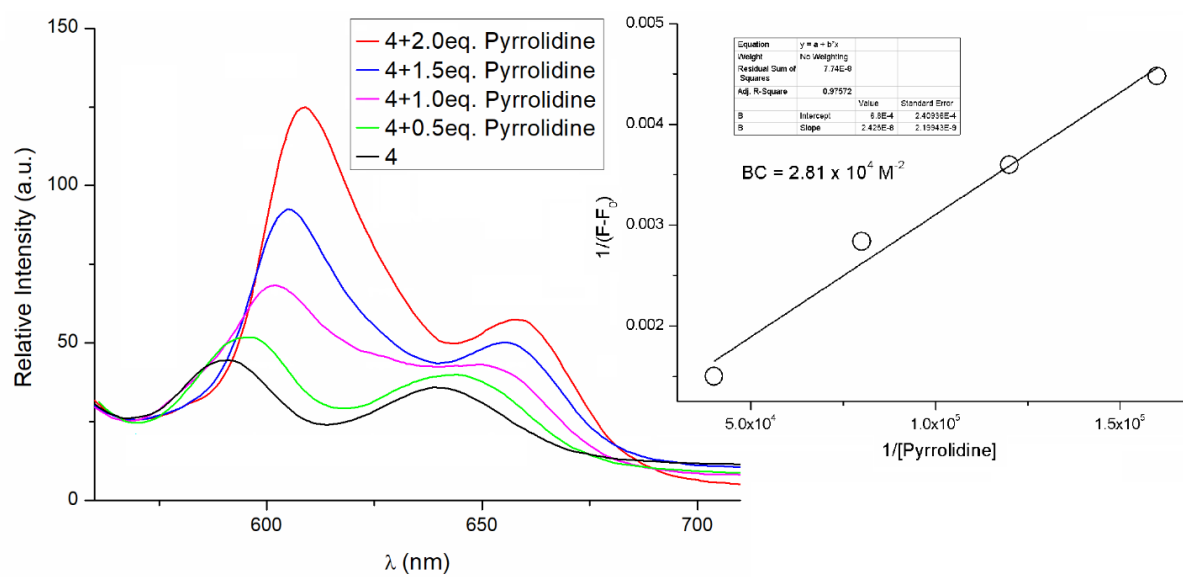


Figure S17. Fluorescence intensity changes of triad **4** upon the addition of pyrrolidine in CHCl_3 .

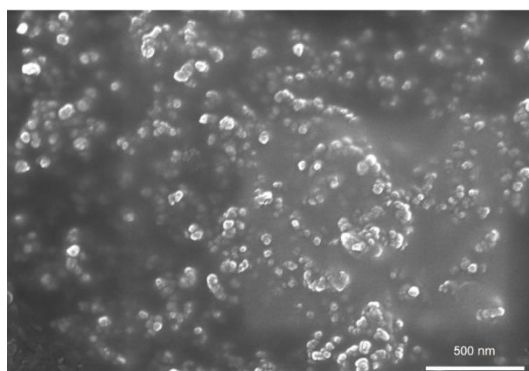


Figure S18. SEM image for the aggregates of triad **4** upon the addition of pyrrolidine.

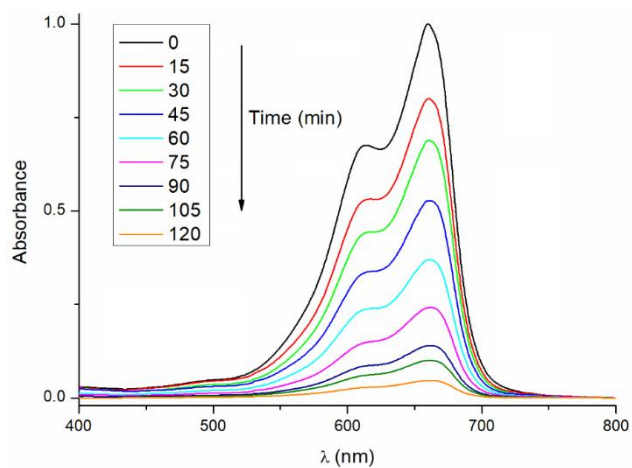


Figure S19. Absorption spectra of MB in presence of nano fibers derived from triad 4 under visible light irradiation.

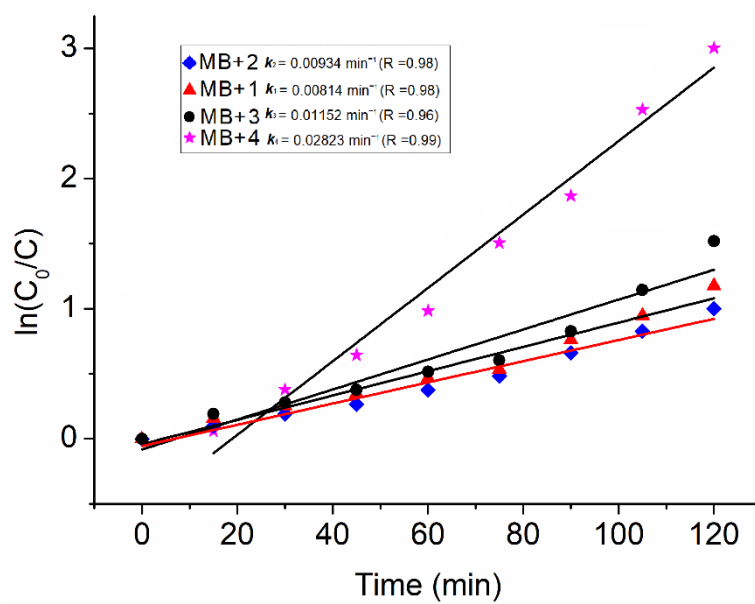


Figure S20. Kinetics for the photocatalytic degradation of MB under visible light irradiation of the four triads (1, 2, 3, and 4).

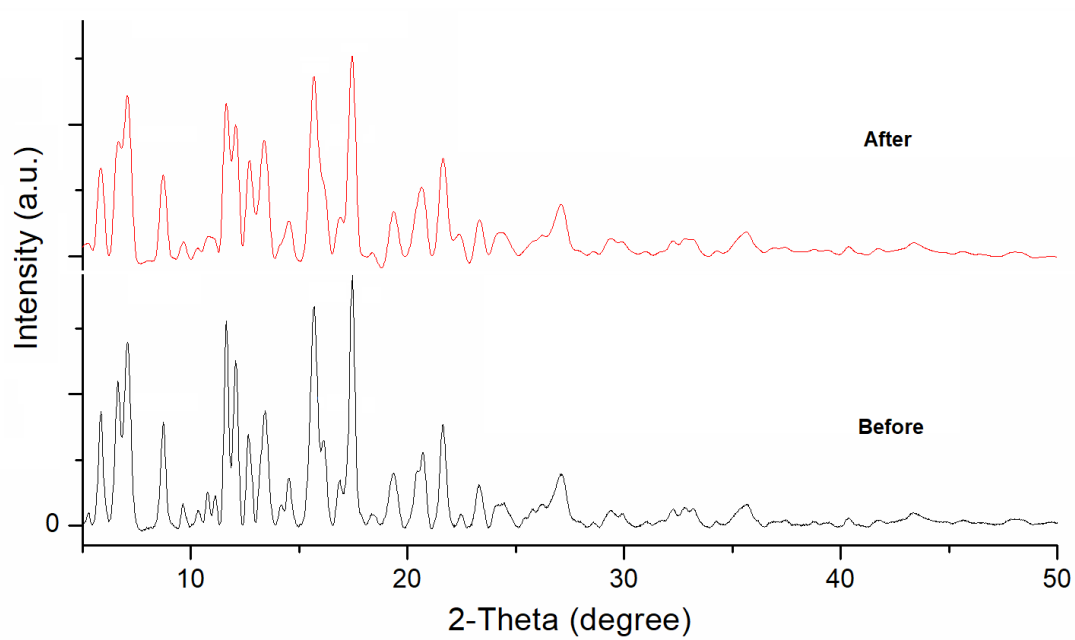


Figure S21. PXRD data of triad **4** before and after an experiment on the photo-degradation of MB.

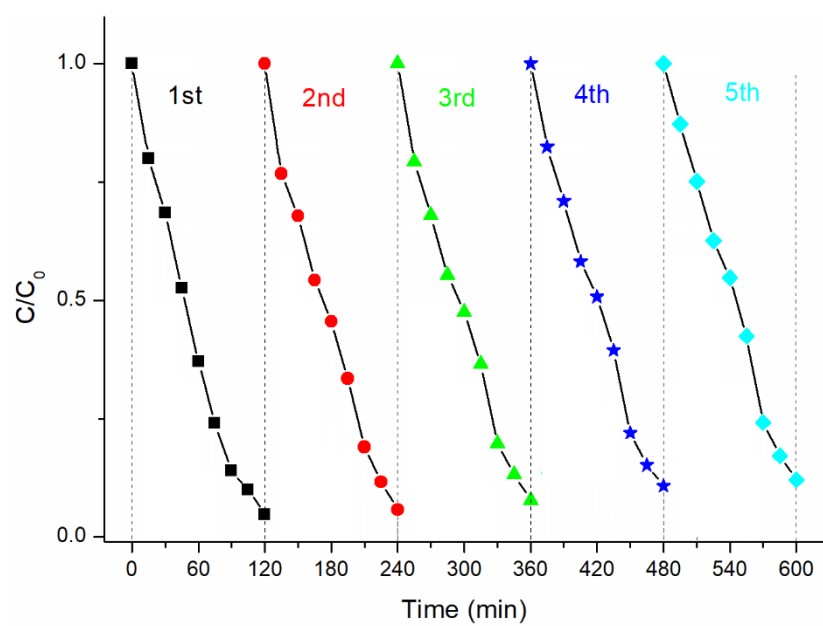


Figure S22. Catalytic cycles using triad **4** as a photocatalyst for the degradation of MB.